MICHIGAN STATE UNIVERSITY

CYCLOTRON LABORATORY

CRITICAL PHENOMENA AT LOW TEMPERATURE

DAVID K. SCOTT

INVITED TALK PRESENTED AT
SIXTH HIGH ENERGY HEAVY ION STUDY AND
SECOND WORKSHOP ON ANOMALONS
LAWRENCE BERKELEY LABORATORY, JULY 1983

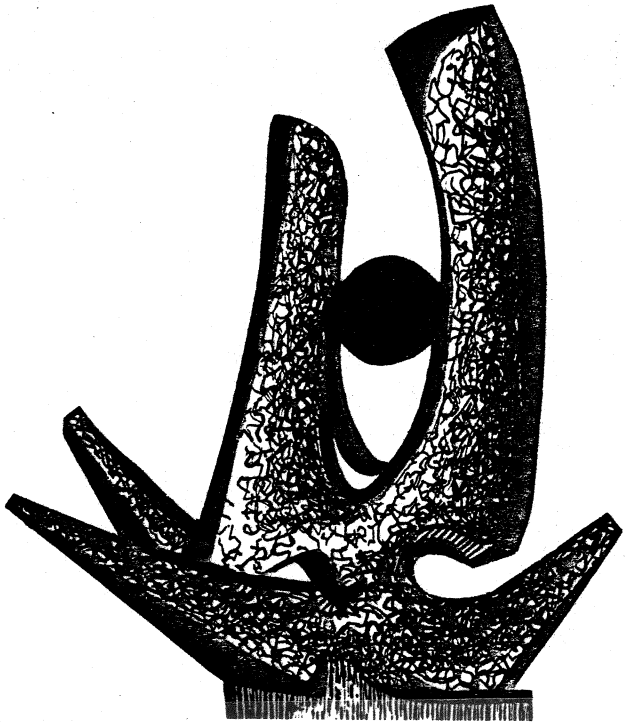

SEPTEMBER 1983

MSUCL 434

MSUCL 434
September 1983

CRITICAL PHENOMENA AT LOW TEMPERATURE

David K. Scott

National Superconducting Cyclotron Laboratory

and

Departments of Physics and Astromony
and of Chemistry
Michigan State University
East Lansing, Michigan 48824, USA

CRITICAL PHENOMENA AT LOW TEMPERATURE

Phenomenology cannot represent Nature without transgressing experience . . . . Experience, says Goethe, is always only half experience

(L. Boltzmann, On the Evolution of the Methods of Theoretical Physics in Recent Times, 1899)*

Abstract

Critical phenomena in high energy heavy ion collisions have long been of interest in view of the possibility of creating new states of nuclear matter in the form of a pion condensate, density isomer, and a quark-gluon plasma. In this paper we discuss critical phenomena which may be relevant at much lower densities and temperatures. Instabilities associated with a liquid-gas phase transition and a nuclear break-up when the compressibility becomes negative are discussed. Although the phenomena are less exotic than those conjectured to occur at high density or temperature, they also rely for their evolution on a hydrodynamical description of nuclear collisions. Questions of time scales, which are important for all types of critical phenomena, are touched upon. Some of the possible experimental signatures, along with present evidence, for the onset of critical behavior are described. A discussion of more general implications of the behavior of the nuclear equation of state at low density and temperature is included. Low temperature critical phenomena have implications on topics as diverse as the nuclear mean free path, anomalons, and the evolution of supernovae.

1. Introduction

The possibility of creating states of matter resembling those prevailing in the early Universe constitutes a major incentive for the study of high energy heavy ion collisions.[1-3] If energy densities of 2-4 GeV/fm^3 can be achieved, then according to quantum chromodynamics, a phase transition to a quark-gluon plasma may occur. Such a transition represents an extreme example of a critical phenomenon which may exist at high temperatures and densities. Many questions on reaching such a state can be raised--whether, for example, there is sufficient time for the phase transition to manifest itself in the brief time

---

*This quotation was brought to my attention by J.E. Sedlak in the thesis "Nuclear Hydrodynamics with Viscosity and Heat Conduction," University of Wisconsin--Madison, 1982.

during a nuclear collision when high compressions are thought to be reached, and whether phase equilibrium can be sustained by a finite system consisting of a small number of particles. It is of interest, therefore, to explore the consequences of other critical phenomena, which may set in at lower temperatures and densities and which may be attainable with existing accelerators.

In this paper some of these low temperature critical phenomena are explored, viz a fast mechanical instability leading to the break-up of a nuclear system into fragments, and a slower chemical instability involving a transition between gas and liquid phases. Both phenomena rely for their development on a hydrodynamical description of nuclear collisions, and raise issues which may be germane to phase instabilities of more exotic kinds, such as the quark-gluon plasma and pion condensation.

The next section of the paper describes the underlying physics of the instabilities, and is followed in Section 3 with a discussion of the relevant time scales for the processes to be established. Some of the present experimental evidence is discussed in Section 4; more general consequences of the phenomena in the field of heavy ion science are touched upon in Section 5, and the paper in concluded with a summary in Section 6.

Since at present the theoretical prediction of the experimental consequences has only been developed in a phenomenological way, and since few experiments have been carried out at the level of sophistication necessary to confirm the existence of these phase instabilities, the quotation at the beginning of this section--taken from the work of Boltzmann--is therefore quite apt.

2. Critical Conditions at Low Temperature

An accepted picture of high energy heavy ion collisions is shown on the right of Figure 1 and illustrates the division of a reaction in the participants and spectators.[4] This behavior is established in nuclear collisions at high energies and is to be compared with the slower, more gentle, evolution associated with the TDHF description shown at the left. We shall assume that the participant-spectator description is valid at energies of 50-100 MeV/nucleon. (Some justification for this assumption will be presented in Section 6.) The participant zone is initially compressed and heated; during the subsequent expansion, when the density and temperature drop, it is possible that the system passes through conditions favorable to a division into liquid and gaseous phases, thereby influencing the production of complex fragments. Although frequent discussions of this phenomenon have appeared in the literature (see, for example, Refs. 5-7) pertaining to the evolution of neutron stars and supernovae, its possible manifestation during the dynamical evolution of a heavy ion collision has only recently been raised.[8-13] In the following, a simplified analytical treatment is followed to illustrate the basic ideas; more formal treatments can be found in the above references.

Consider the following parameterization of the energy per particle, E, in a nuclear system as a function of temperature, T, and density, ρ;

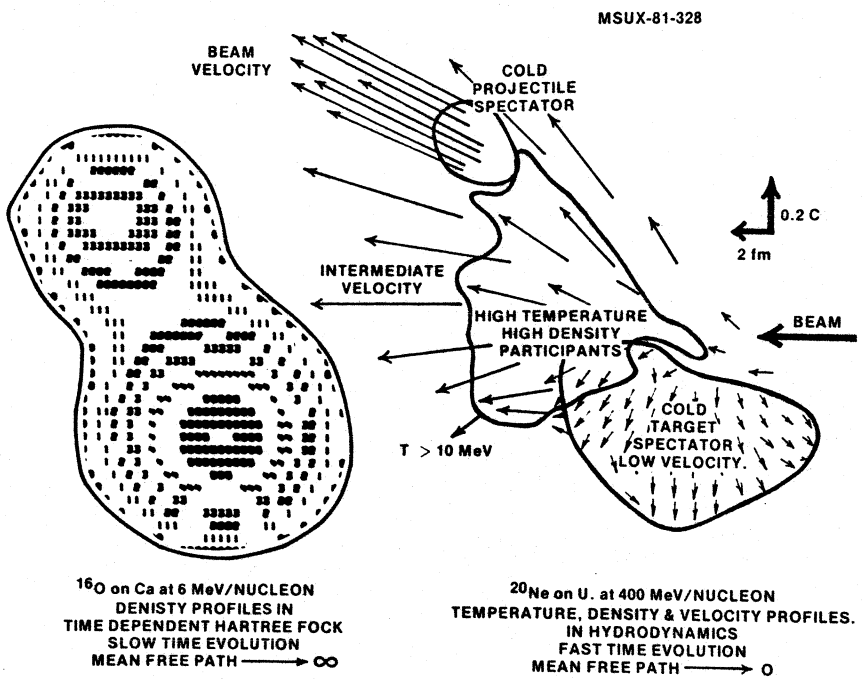

Figure 1. The participant-spectator picture of high energy heavy ion collisions is illustrated at the right by temperature and density profiles calculated with a hydrodynamical model. The participant zone initially contains high density and high temperature nuclear matter. This view of a reaction is contrasted with the picture obtained from a TDHF calculation at low energies shown on the left.

$$E = E_0 + \frac{K}{18}\left(\frac{\rho-\rho_0}{\rho_0}\right)^2 + \frac{\pi^2}{4\varepsilon_F} T^2 \left(\frac{\rho_0}{\rho}\right)^{2/3}$$

which is comprised of the ground state binding energy per particle E_0, the compressional term containing the incompressibility K, and a thermal contribution derived from the low temperature approximation for a Fermi gas; ε_F is the Fermi energy and ρ_0 the normal nuclear matter density of approximately 0.16 nucleons/fm^3. From the free energy F = E - TS, with the specific entropy

$$S = \frac{\pi^2}{2\varepsilon_F} T \left(\frac{\rho_0}{\rho}\right)^{2/3} ,$$

we obtain

$$F = E_0 + \frac{K}{18}\left(\frac{\rho-\rho_0}{\rho_0}\right)^2 - \frac{\pi^2}{4\varepsilon_F} T^2 \left(\frac{\rho_0}{\rho}\right)^{2/3} .$$

The pressure as a function of ρ and T can be calculated from,

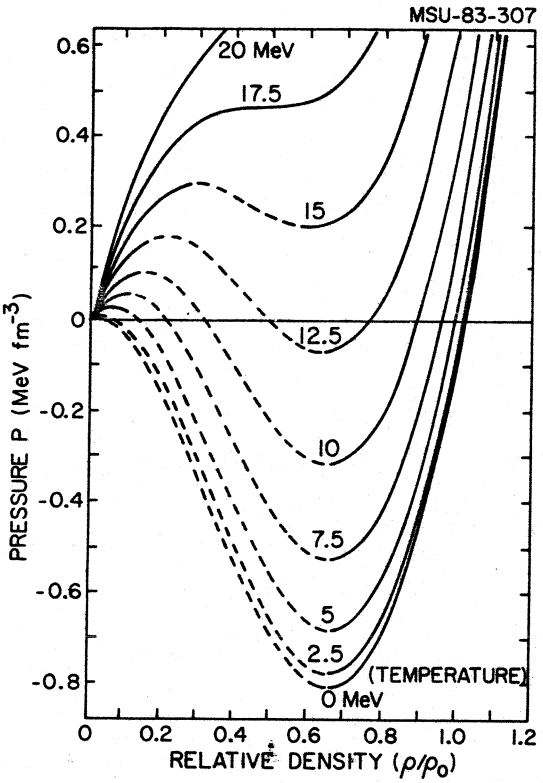

Figure 2. The equation of state for a nuclear system is illustrated by isotherms for pressure versus density. The isotherms separate into two regions which can be identified with liquid and gas phases in a Van der Waals system, connected by a region of negative incompressibility (shown dashed).

$$P = \left(\frac{\partial F}{\partial V}\right)_T = \rho^2 \left(\frac{\partial F}{\partial \rho}\right)_T$$

Results for a more complete calculation[5] are shown in Figure 2, where it can be seen that the equation of state has the form of a Van der Waals system, for the simple reason that the nuclear and molecular systems are analogous; both are subject to short range attractive forces and very short range repulsions.

As in the Van der Waals system, there exist liquid and gaseous phases. For the unphysical region (shown dashed in Figure 2) where the slope of P versus ρ is negative (implying a negative incompressibility) a Maxwellian construction is employed, along which the liquid and gas phases coexist. This region of coexistence is illustrated[11] more clearly in Figure 3, which also shows that as the temperature increases, the apex of the coexistence region coincides with the inflection point of the critical temperature. This point corresponds to the condition,

$$\frac{\partial P}{\partial \rho} = \frac{\partial^2 P}{\partial \rho^2} = 0$$

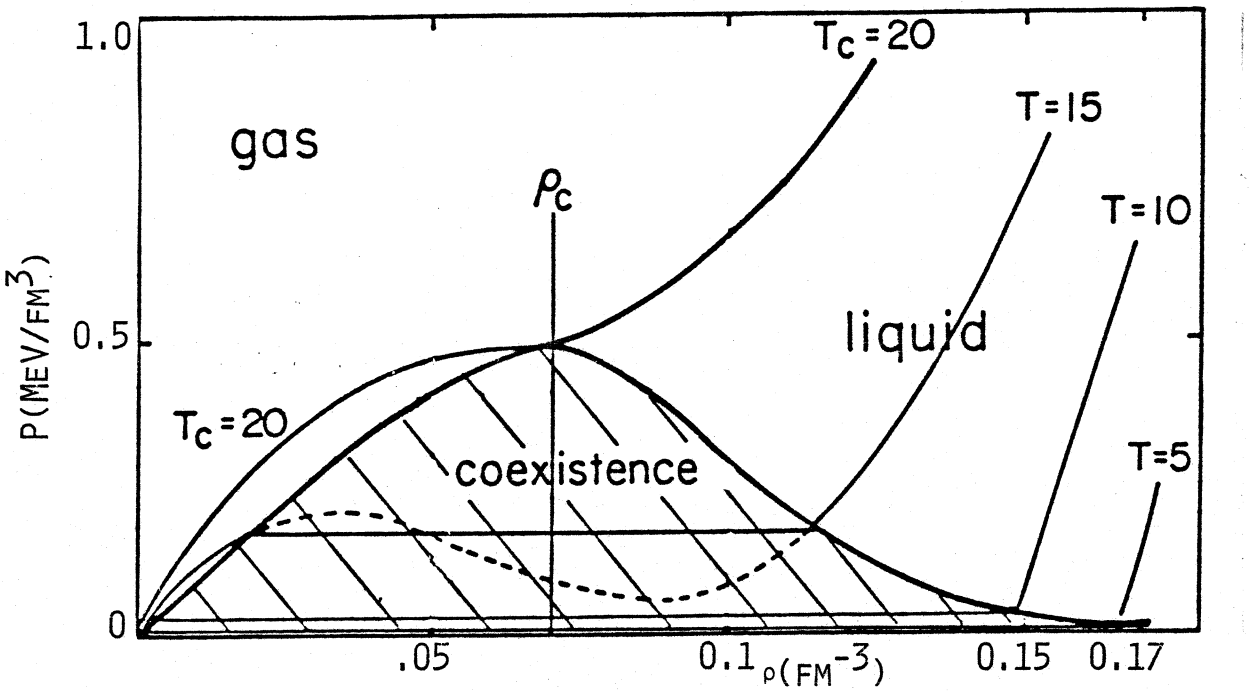

Figure 3. Pressure-density isotherms in which the region of negative compressibility is suppressed (compare Figure 2) by the Maxwell construction describing a phase transition between liquid and gas. The region of phase coexistence is shown by the cross hatching. Above T = 20 MeV only a single gas phase exists irrespective of the density. The critical density is 0.065 fm^{-3}.

A solution of the above analytical expressions with K ≅ 210 MeV, consistent with measurements of the monopole excitation, gives a result close to that obtained from a more detailed analysis, viz $T_c \cong 18$ MeV and $\rho_c \cong 0.07$ nucleons fm^{-3}. For all higher temperatures only a gaseous phase exists.

Most studies of heavy ion collisions at relativistic energies have been conducted in regions where the temperature exceeds 20 MeV. In the later discussion on observable consequences we shall show that temperatures for the participant zone of 20 MeV and lower are generated in collisions below 100 MeV/nucleon, implying that intermediate energy heavy ion studies will be most important for the investigation of these critical phenomena.

Another type of instability, which would occur on a faster time scale than the liquid-gas transition, has also been discussed recently.[14] This concerns a mechanical instability where the compressibility of the nuclear system $K = \rho \frac{\partial P}{\partial \rho}$ becomes negative. Such a region is easily identified in Figure 2 by the dotted lines, but is shown more clearly in Figure 4 where K is plotted as a function of density for different temperatures. The region of zero or negative compressibility falls below the horizontal axis. The corresponding boundary is transposed onto the plot of internal energy as a function of density in Figure 5. Here the region labelled "unstable zone" defines where nuclear matter becomes dynamically unstable. Expressed alternatively the boundary traces out the locus of the tensile stress of nuclear matter as a function of temperature. The authors of Ref. 14 argue that the occurrence of nuclear fragmentation as a dominant reaction process depends on whether the system enters

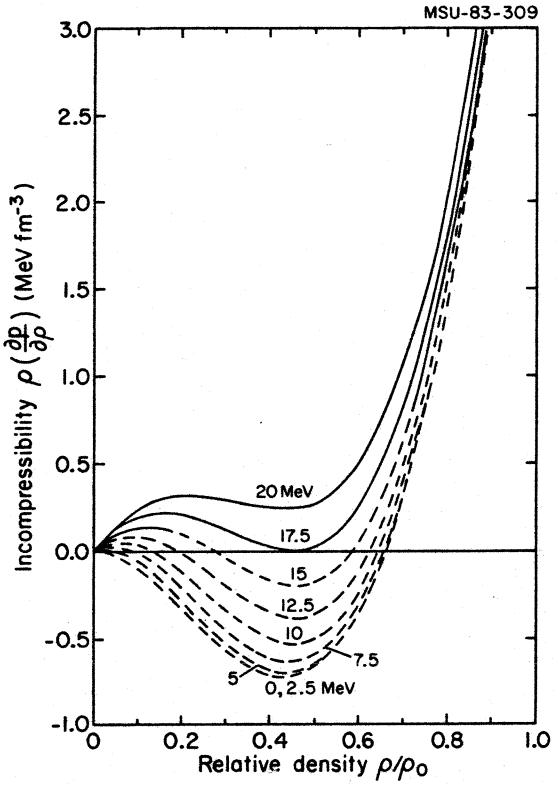

Figure 4. The rigidity $\rho \frac{\partial P}{\partial \rho}$ plotted as a function of density for various temperatures. The region of negative incompressibility, shown dashed in Figure 2, corresponds to the part of the diagram below the horizontal axis. The rigidity of the liquid is much larger than that of the gas.

this unstable region. Since the zone has a boundary of lower than normal nuclear matter density, it is necessary to consider how it can be reached, given that a nuclear system is prepared in a reaction at normal or greater than normal density.

The region labelled "overstressed zone" on Figure 5 defines a boundary which will under certain conditions allow the system to reach the unstable region. Initially a nuclear reaction carries the system from the ground state to some point with higher internal energy. If the energy is transferred by a proton, it is plausible to assume that no significant compression takes place. On Figure 5 the system moves vertically upwards on the diagram from the minimum at normal nuclear density, requiring an injection of approximately 10 MeV per particle. On the other hand, for heavy ion collisions we expect some compression to occur, which prepares the system initially at a point to the right of the minimum of normal density. From this condition it is assumed that the nuclear system will expand along an isentrope until a point of equal internal energy is reached on the left. The justification for an expansion at constant entropy is based on cascade calculations,[15] which indicate that little dissipation takes place; other evidence comes from our knowledge of the monopole vibration, which has a damping width much smaller than its excitation.[16] In Figure 5 the region of appropriate initial conditions which will provide access to the fragmentation zone is defined by the dashed boundary of the shaded region

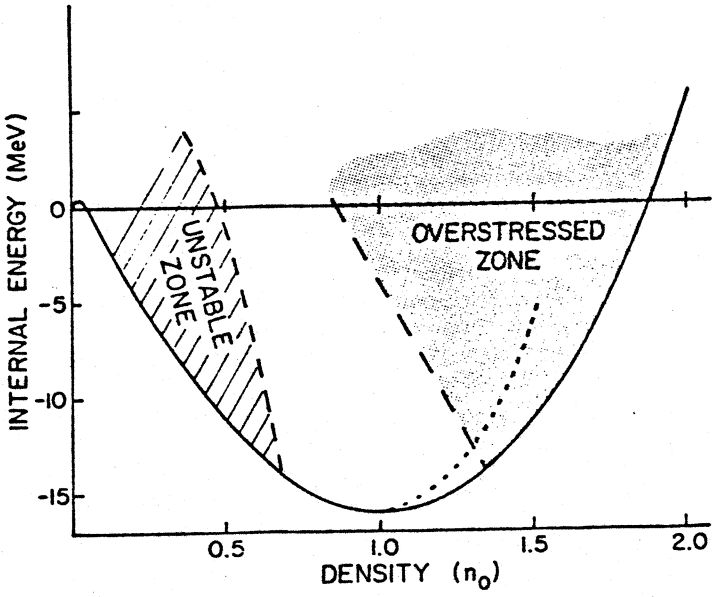

Figure 5. The internal excitation energy per nucleon is shown as a function of relative density. The shaded portion on the left, labelled "unstable zone", defines the region of negative incompressibility. The shaded area on the right defines the overstressed zone from which a nuclear system will be able to reach the unstable zone through an isentropic expansion. The dotted locus extending into the overstressed zone indicates the trajectory expected from theoretical calculations of heavy ion collisions.

labelled "overstressed zone". For example, a compression of 1.4 over normal density is predicted[17] in TDHF calculations at 10 MeV/nucleon (see the dashed line to the left of the S = 0 isentrope in Figure 5), and if it is assumed that all of this excitation energy is thermalised, then the threshold for fragmentation would be lowered to 3 or 4 MeV/nucleon. The corresponding incident energy in the laboratory, assuming again equal participation from target and projectile, would be in the region of 12 MeV/nucleon. Above this threshold the system will always come apart in fragments. An observation of the onset of fragmentation might therefore provide a means of inferring the density at which thermalization takes place; the energy threshold for fragmentation should be an increasing function of the initial density. We shall return to this predicted behavior in Section 5.

3. Time Scales

The mechanical and chemical instabilities we have discussed are quite different in nature. One is a first order transition applicable to processes that occur slowly enough for an equilibrium to be established across the phase boundary. According to the picture of expansion and rarefaction of the initial compressed zone on a time scale commensurate with the frequency of the monopole vibration, this time can be estimated from the typical excitation energy in a

medium weight nucleus,[15] $E \cong \hbar\omega \cong 15$ MeV, resulting in an expansion time of the order 10^{-22} sec. This time scale is the relevant one for a mechanical instability. It is not clear, however, if a liquid-gas chemical instability can be established on this short time scale, since there must exist sufficient time for equilibration to be established across the phase boundary. The time required for this equilibration to occur is of the same order as the evaporation time, an estimate of which can be obtained from the theory of thermionic emission.[18] Thus the current density can be expressed as

$$J = \frac{em}{2\pi^2\hbar^3} T^2 (1 - r) e^{-W/T}$$

where r is the quantum mechanical reflection coefficient (taken as 0), W is the work function (taken as 8 MeV) and T is the temperature. By definition

$$J = \frac{\Delta q}{\Delta t} \frac{1}{A}$$

where A is the surface area of the emitting source. If we set q = e (equivalent to the emission of one nucleon) then $\Delta t = \tau_{evap}$. Assuming a spherical geometry, so that $A = 4\pi R^2$ where $R \cong 3.5$ fm. as determined from the participant-spectator model for intermediate impact parameters[19] and consistent with determinations from pion interferometry measurements,[20] the evaporation time is found to be

$$\tau_{evap} \cong 3.5 \times 10^{-21} \cdot \frac{1}{T^2} \cdot e^{8/T} \text{ sec.}$$

The resulting values given in Table 1 are in good agreement with results deduced from an empirical fit to the measured widths of compound nuclei for A = 20 - 100.[21] Comparing the evaporation time with the time required for disassembly it appears that for $T \gtrsim 8.1$ MeV (henceforth referred to as the breakeven temperature) the liquid-gas phase instability may develop.

Table 1. Nucleon evaporation times as a function of temperature.

T (MeV)	5	10	15	20
t (10^{-22} sec)	6.9	0.77	0.27	0.13

Since a liquid-gas phase instability exists only for temperatures below the critical temperature and above the breakeven temperature, it is obvious that if the breakeven temperature were higher than the critical temperature, the liquid-gas instability would not develop. The critical temperature of approximately 20 MeV predicted in Refs. 10 and 11 was deduced on the assumption that the binding energy per nucleon in nuclear matter is 16 MeV/u compared to the phenomenological binding energy per nucleon of 8 MeV for finite nuclei. A more thorough treatment of this question and of effective mass considerations is given in Ref. 12, where it is shown that in finite nuclei the predicted critical temperature lies between 13.4 MeV and 8.1 MeV depending on the choice

of effective mass. Thus for temperatures above 8 MeV the liquid-gas instability may develop and there is sufficient time for it to do so.

Collision damping has been neglected throughout this discussion. A simple approach[22] to the problem begins with the equation for a damped non-driven oscillator:

$$\ddot{x} + \gamma\, x + \omega_0^2\, x = 0$$

$$x = \rho - \rho_{min}\ (S)$$

$$\Gamma = \frac{\gamma}{\omega_0^2 - \frac{1}{4}\gamma^2}$$

where γ is the damping coefficient (assumed constant) and ω_0 is the undamped harmonic oscillator frequency. The dimensionless damping coefficient can be deduced from experimental measurements of the monopole oscillation characteristics. The variable ρ_{min} is the value of the density when the excitation energy is a minimum for a given value of the entropy. The damping constant determines the rate at which energy is transferred to thermal energy from the collective motion, thus determining the temperature. For a given value of the density, the entropy can be calculated and ρ_{min} can be determined. Although the oscillation in the density coordinate is not a true harmonic motion we shall use this approximation for small excursions from the equilibrium density. A solution to the above equation is of the form,

$$x \cong Ae^{-\gamma t/2}\cos(\omega t)$$

where

$$\omega^2 = \omega_0^2 - \frac{1}{4}\gamma^2$$

The time required for disassembly is then

$$t \cong \frac{\pi}{\sqrt{\omega_0^2 - \frac{1}{4}\gamma^2}}$$

The empirical full width at half maximum (FWHM) of the monopole excitation is typically $\cong$ 4 MeV for an excitation energy of 15 MeV.[23] Table 2 illustrates how values of the damping constant influence the breakeven temperature for the onset of the liquid-gas instability. In Figure 6 the overstressed region is redefined assuming that the damping constant remains fixed at $\Gamma = 0.27$ (indicative of $T = 0$ damping) and is not a function of temperature. The minimum

Table 2. Breakeven temperatures for various values of the dimensionless damping constant.

$\Gamma/\Gamma\ (T \cong 0)$	0	5	10	20
$T_{breakeven}$ (MeV)	8.1	7.6	6.9	5.8

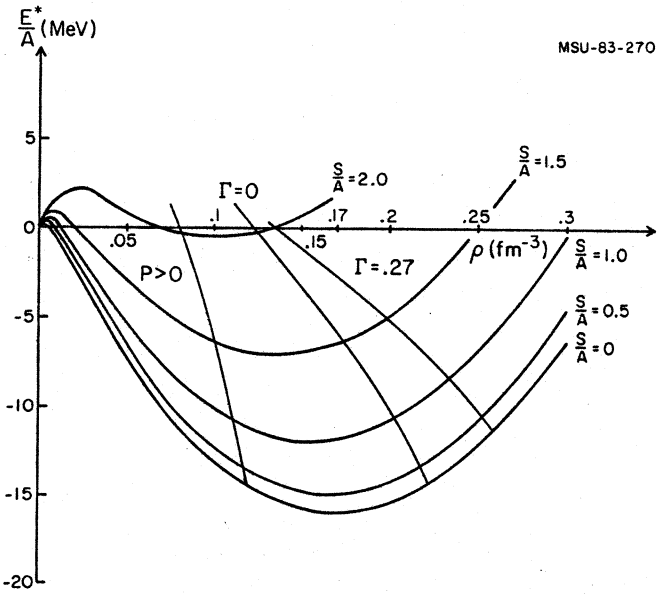

Figure 6. Compared to Figure 5, this figure shows two determinations of the boundary of the overstressed zone. One, labelled $\Gamma = 0$, is identical to that of Figure 5, and the other, $\Gamma = 0.25$, takes into account damping effects during the expansion, increasing the threshold energy for reaching the unstable zone.

excitation energy of the overstressed region becomes 4.75 MeV above the binding energy of normal nuclear matter (E = -16 MeV) with $\rho \cong 1.5$ times normal nuclear density. For an equal mass of projectile and target the minimum incident energy required is 4 times the excitation energy, i.e. approximately 19 MeV per nucleon. If this incident energy is insufficient to generate a compression of 1.5 times normal nuclear density, then the minimum required energy will be even larger.

4. Experimental Consequences

The great tragedy of Science--the slaying of a beautiful hypothesis by an ugly fact

T.H. Huxley, Collected Essays

So far there have been few experiments specifically directed at observing the influence of low energy critical phenomena. In this section we review some of the types of data which may be relevant. It is well known that in high energy proton-induced spallation the cross section for fragment production increases dramatically up to energies of a few GeV, followed by a levelling off in the cross section. An example[24] is illustrated in Figure 7 for p + Ag leading to ^{24}Na. The saturation is usually attributed to a limitation of the energy deposition in the nucleus when it becomes transparent to protons of a few GeV. On the other hand, the behavior may be related to the onset of fragmentation when the system reaches the overstressed region.[14] For the system

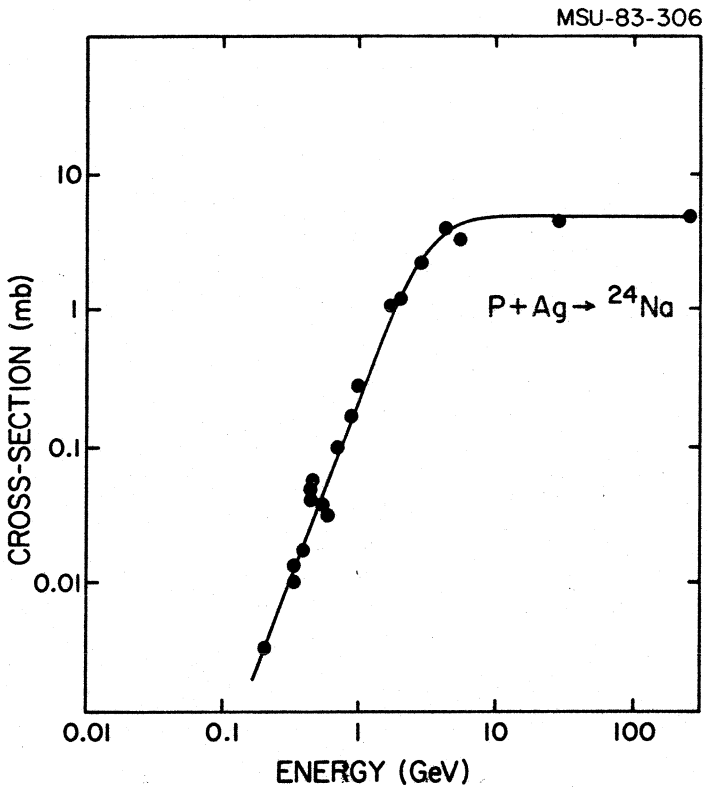

Figure 7. The cross section for the production of ^{24}Na in spallation reactions induced by protons on Ag as a function of incident energy. Following a rapid rise, the cross section saturates at energies above 2 GeV.

p + Ag with about 108 nucleons, our previous discussion would imply that about 1 GeV of energy is necessary. Of clear interest here would be a comparison with heavy ion induced fragmentation in order to discover if the saturation sets in at a lower energy in the presence of some compression. A preliminary comparison of this type is shown[25] in Figure 8, from which there is some indication that a lower threshold may indeed exist in heavy ion proton induced reactions leading to the production of ^{24}Na and Sc isotopes with a Au target.

We should also point out that other approaches to high energy proton induced break-up of a target have recently been discussed; for example,[26] in the process of "cleavage" a high energy proton drills a hole through the nucleus and when the hole expands bonds are broken to release the observed nuclear fragments. A simple argument can be used to show that the energy per particle released in this process may be considerably smaller than the estimate of the energy of 10 MeV/particle required to access the overstressed zone. The cleavage model does appear to give a satisfactory descripton of the absolute production cross sections and energy distribution of the fragments, although so far it has mainly been applied to more massive fragments than have been explained by the models of critical phenomena.

At very high proton energies of 30-350 GeV, the proton induced data have also been interpreted in terms of critical phenomena associated with a liquid-

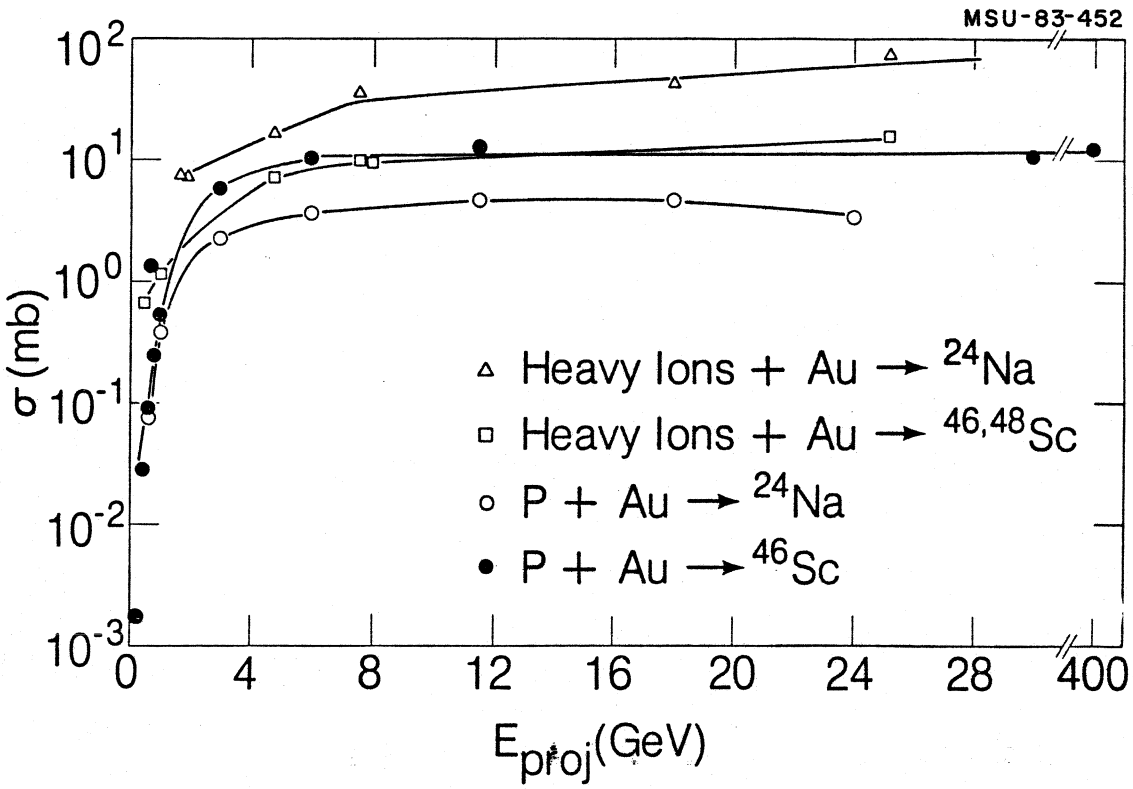

Figure 8. A comparison of yields of ^{24}Na and ^{46,48}Sc in proton and heavy ion induced reactions. There are some indications for differences in the energy at which saturation sets in.

gas phase transition.[27,28] The observation that the mass yield of fragments obeys a power law in fragment mass number, A_F, viz

$$Y(A_F) \propto A_F^{-\tau}$$

with $\tau \cong 2.6$ is taken as a signature for fragment formation near the critical point. According to the theory of condensation in gases and liquids developed by Fisher,[29] this power law describes the size distribution of resulting droplets, and τ is predicted to have a value in the interval $2 < \tau < 3$. An example of the distribution of fragments fitted with this power law is shown in Figure 9, using an exponent of 2.34. Values of the critical density are found to be $\cong \rho_0/2$ in this study; the extracted critical temperature, $T_C \cong 4$ MeV, is, however, well below the value of 17.5 MeV mentioned in Section 2. We recall that this value was appropriate for the case of infinite nuclear matter. When a more complete treatment of effective mass and binding energy corrections are included the value of T_C is lowered[12] to the region 8-13 MeV, but it is still much higher than 4 MeV. We must note, however, that there are difficulties in extracting temperatures from the experimental data, since the values obtained from the distribution of isotopes and energies differ.

The pure power law form applies strictly only at the critical temperature. Following the treatment of Siemens,[30] one can write in general that the

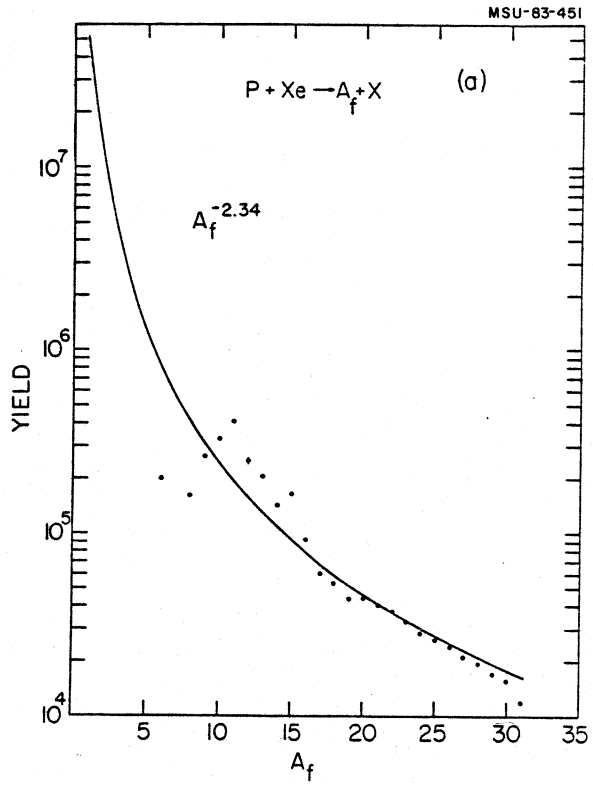

Figure 9. Yield of fragments from the reaction P vs. Xe, typical of the incident energy range from 80 to 350 GeV. The line describes a power law dependence $A_F^{-2.34}$ indicative of critical phenomena of condensation.

probability P_A of finding a cluster A in the fluid is given by

$$P_A \propto A^{-\tau} \exp[-b(T)A^{2/3}]$$

where $b(T) = 4\pi r_0^2(T) \frac{\sigma(T)}{T}$ with $\sigma(T)$ the surface energy coefficient. At zero temperature $\sigma(T)$ takes the value of 1.14 MeV/fm^2, familiar from the liquid drop mass formula. As the temperature is increased the liquid density approaches the critical density of about 0.065 nucleons per fm^3; since the gas density also approaches the critical density, the density difference at the interface vanishes and the surface energy approaches zero.

In Figure 10 a calculation of the surface energy as a function of temperature is shown[31] for three values of compressibility, where the nuclear potential energy is treated within Breuckner's energy-density formalism with appropriate corrections for surface and asymmetry effects. We see that for $K \cong 230$, close to values of the compressibility derived from measurements of the monopole excitation, σ is predicted to vanish at $T \cong 12$ MeV. A rather similar value is obtained by Sauer et al.[32] who parametrize the surface energy coefficient by

$$\sigma = 1.09(1 - 7.16 \times 10^{-3}T^2) \text{ MeV fm}^{-2}$$

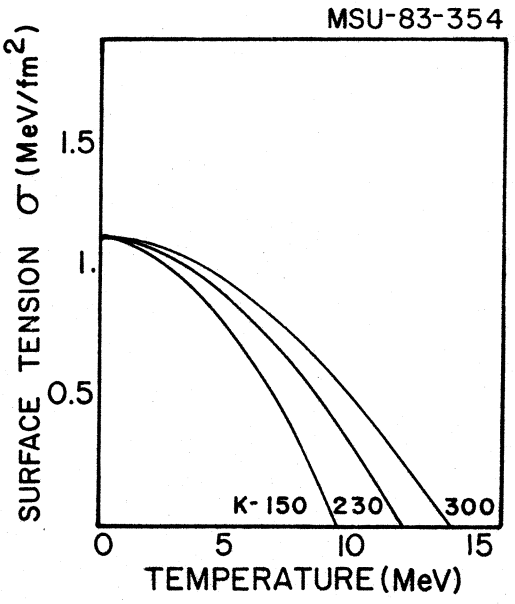

Figure 10. The surface tension σ as a function of temperature for several ground state compressibilities.

which reaches zero at 11.82 MeV. It is encouraging that these deviations result in critical values of the temperature in rather close agreement with the values deduced from studies of the critical temperature of the liquid-gas phase instability in finite nuclei. The consistency implies that studies of fragment production as a function of energy could add to our knowledge of the temperature dependence of nuclear parameters such as the surface energy coefficient. The expected A dependence[30] of the cross section for values of the temperature below near and above the critical temperature are shown in Figure 11. In this calculation a critical exponent of 2.0, a temperature of 8 MeV, and a surface coefficient of 10 MeV were used for $T < T_c$. The dotted line for $T > T_c$ gives a more rapid fall-off as would be predicted, for example, by the coalescence model.[33] In this model the production cross section of a fragment of mass A depends on the A^{th} power of the single nucleon cross section, giving rise to a steeper A dependence than in the expression for $T = T_c$.

In order to determine the incident energies required in a heavy ion collision to reach temperatures appropriate to the instabilities, we refer to Figure 12 which gives values of temperature derived from a study of particle emission from the participant zone of local high temperature and high density nuclear matter. The temperatures were extracted[34] from the energy spectra of emitted light fragments ranging from protons to ^{12}C in reactions induced by incident projectiles from α particles to Argon. Spectra were fitted with a "moving source model", characterized typically by a velocity half the projectile velocity, i.e. a source of intermediate rapidity such as would be expected if projectile and target contribute roughly equal numbers of nucleons to the formation of the hot zone. At high energies of several hundred MeV/nucleon and above, direct evidence for the existence and size of such a localized zone comes from experiments on two-particle interferometry.[19,35] Although no such convincing proof is yet available at intermediate and low energies, we shall

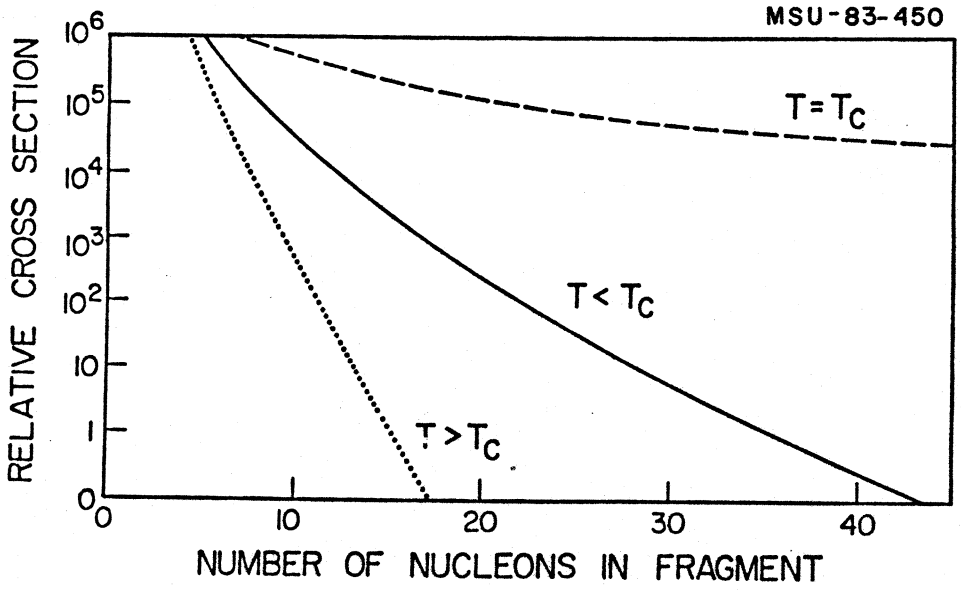

Figure 11. Expected dependence of cross sections on fragment mass A for temperatures above (dotted line), at (dashed line), and about half (full line) the critical temperature T_c. The critical exponent used was 2.0, the surface coefficient was 10 MeV, and the temperature was 8 MeV for the full line (see Ref. 30 for details).

also make use of the results of Figure 3 for the temperature as a function of incident energy.

In part justification we note that the trend of temperatures in Figure 3 is roughly that expected for a Fermi system composed of equal numbers of projectile and target nucleons. Thus, if we write the expression for temperature in a Fermi system as $E^* = T^2/16$, where E^* is the excitation energy per particle and the factor 1/16 comes from the level density parameter, then the result $E = 1/4\ (E_L/A)$ follows, where E_L/A is the incident laboratory energy per particle. Then $T = 2\sqrt{E_L/A}$, and for $T \cong 20$ MeV we obtain $E_L/A = 100$ MeV/nucleon in agreement with the experimental result. Temperatures below the critical value of 18 MeV are therefore appropriate to collisions below 100 MeV/nucleon, placing the observation of the liquid-gas phase instability in the intermediate energy regime.

A power law distribution of fragment cross sections has been found to apply in several other reactions, as for example[36] in the reaction of ^{12}C on Ag at 30 MeV/nucleon, shown in Figure 13. Here the dashed line corresponds to $\sigma_Z \propto Z^{-2.6}$; Z is the charge of the fragment and is roughly proportional to the mass. The authors of this work estimate an upper bound for the temperature reached in the reaction of about 12 MeV, which is the value appropriate for equal participation of target and projectile nucleons as shown in Figure 12. For reactions of this type, in which fragments much heavier than the projectile are produced, it is quite possible that a much larger volume of the target nucleus participates; the associated temperatures would then be commensurately lower. More detailed systematic studies as a function of incident energy will be required to clarify the situation.

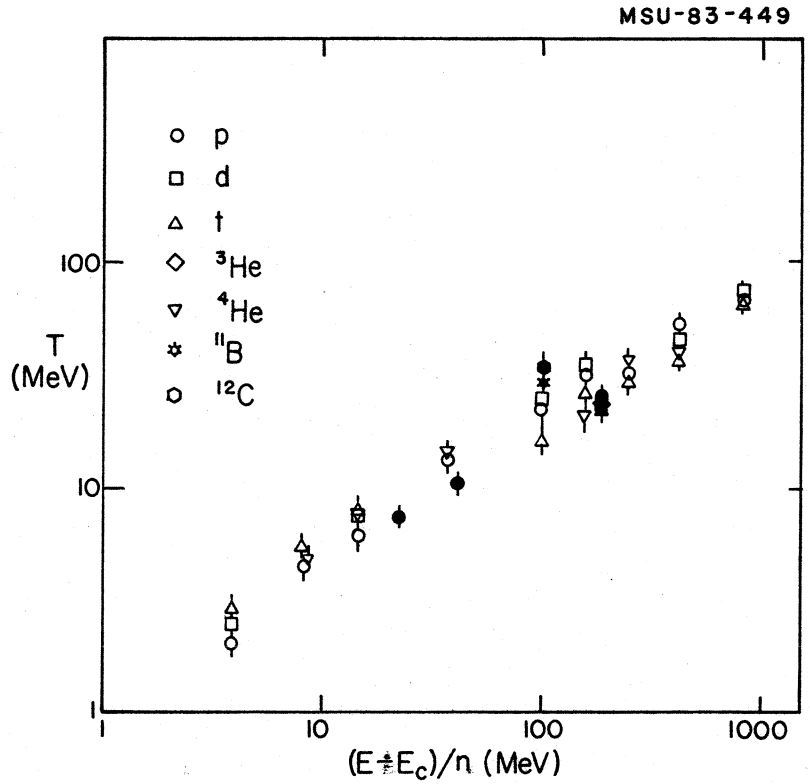

Figure 12. Plot of temperatures as a function of incident energy per nucleon above the barrier, derived from a parameterization of the energy spectra of emitted light fragments with a localized moving source. Results are shown for different emitted fragments p, d, t, ^{3}He, ^{4}He, ^{11}B, and ^{12}C in reactions induced by α, ^{16}O, ^{20}Ne, and ^{40}Ar (see Ref. 34 and references therein for details).

Models which do not explicitly incorporate critical behavior can also be used to explain some aspects of the data we have been discussing. In Figure 13, for example, the data are compared with a statistical model calculation[37] for the idealised case of emission from a completely equilibrated composite system. Isotropic particle emission was assumed, angular momentum effects were neglected, and the level density was assumed to correspond to an ideal Fermi gas at normal density. As indicated by the solid histogram the calculation gives a tolerable account of the data. A similar calculation of the fragment distribution in Figure 9 for high energy proton induced reactions met with comparable success.[38] It bears repeating that only through detailed studies over a range of energies will it be possible to distinguish the different theoretical models, and to confirm the presence of critical phenomena. Other examples of power law behavior are discussed in Refs. 39 and 40.

In the discussion of mechanical instabilities we made use of the cascade result that entropy stays fairly constant during the expansion and cooling of the participant zone. Applying this concept also to the case of a liquid-gas phase instability leads[13] to Figure 14, in which the regions of phase mixture and negative compressibility are defined on a pressure-density diagram with lines of constant entropy. For entropies as high as $S/A \lesssim 3$ the isentropic

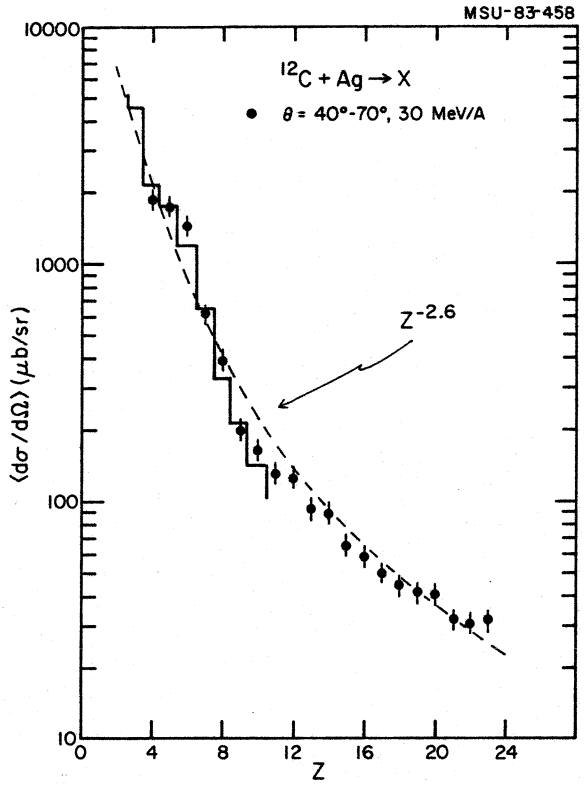

Figure 13. Element production cross sections in the reaction ^{12}C + Ag at incident energy of 30 MeV/nucleon. The dashed line corresponds to a power law dependence $Z^{-2.6}$, and the histogram to a Hauser-Feshbach statistical emission model.

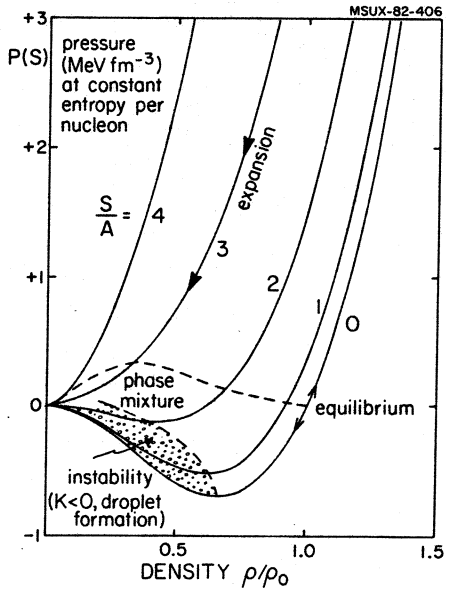

Figure 14. The pressure versus density for a nuclear system as a function of the entropy per particle in the system. The arrows indicate the expansion at constant entropy of the initial compressed and heated zone. The regions of liquid-gas phase admixture and of negative incompressibility discussed for Figures 2-6 are indicated.

lines intersect the region of liquid-gas phase mixture, implying that effects of this instability may be present up to very high bombarding energies of several hundred MeV/nucleon. Now consider a system prepared with initial compression and heating such that the specific entropy S = 2. During the subsequent expansion the temperature and density will drop such that the entropy

$$S = \frac{\pi^2}{2\varepsilon_F} T \left(\frac{\rho_0}{\rho}\right)^{2/3}$$

remains constant. At the intersection with the phase boundary, if a phase transition takes place, the entropy will no longer stay constant but instead the volume will increase at constant temperature along a locus parallel to the horizontal axis in Figure 14. For a system consisting of nucleons only the entropy increase can be derived from the Sackur-Tetrode equation:

$$\frac{S}{A} = \frac{5}{2} + \ln \left(\frac{n_Q}{\rho}\right)$$

where n_Q is the quantum concentration of nucleons. The entropy change is then[13]

$$\Delta S = \ln \rho_{GAS} - \ln \rho_{LIQUID} .$$

Taking values of ρ from Figure 14 we find an entropy increase of $\Delta S \cong 2$ for the case in point. A measurement of entropy as a function of bombarding energy may therefore be a means of detecting the onset of critical phenomena.

Recently it was suggested that a measurement of the yield of complex fragments can be used to measure entropy.[13] In Figure 15 the results of a quantum

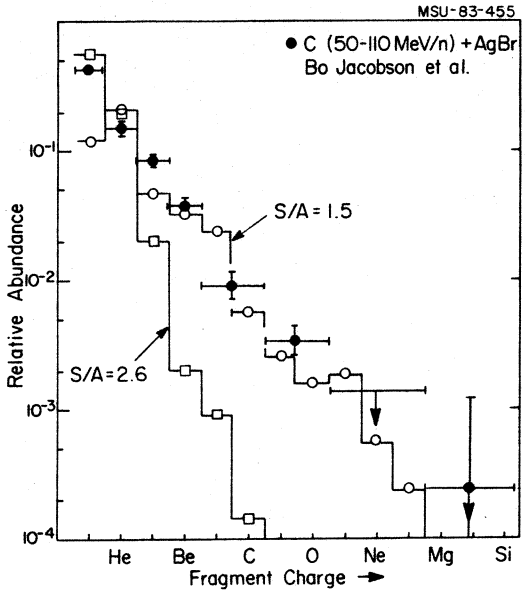

Figure 15. The charge distribution Y(Z) observed in high multiplicity events for the reaction of 50-110 MeV/nucleon carbon in emulsions. The open symbols and histograms are the distributions predicted with a quantum statistical model for two values of the entropy.

statistical model of fragment production are shown for S/A = 1.5 and 2.5. The calculation for S/A = 1.5 is compared with experimental data[41] on complex fragment emission in reactions of ^{12}C in nuclear emulsions at incident energies in the range 50-110 MeV/nucleon. With increasing entropy the yield of heavy fragments decreases rapidly, by two orders of magnitude in the case of nitrogen fragments.

Until recently, emphasis on entropy measurement in heavy ion reactions has focused on the ratio of deuterons to protons emitted from the participant zone, resulting[42] in values which are always in excess of the entropy at the critical point ($S \cong 3.3$, see Figure 14). It may be that such light fragments are produced mainly from a gaseous phase. The comparison with heavier fragments emitted from reactions over a wide energy range will be important for establishing the onset of critical phenomena.

5. More General Consequences

The Fairy Tales of Science and the long result of time

Alfred, Lord Tennyson, Locksley Hall

Apart from the intrinsic importance of the critical phenomena, there may also be other less direct consequences which are of interest. Some of these are discussed in this section.

a) Participant-Spectator Model

As we mentioned in the introduction, the participant-spectator model of nuclear collisions is known to be applicable at high incident energies of hundreds of MeV/nuclei; the limit of validity at low energies is unknown but is of interest, since it relates to the question of localization of the energy deposition in a nucleus. A relevant parameter is the temperature dependence of the mean free path, and the results of one calculation[43] are shown in Figure 16. A rather sudden change takes place in the region of 12 MeV, which has its origin in the change of the transport properties of nuclear matter when considered as a liquid or as a gas. There are corresponding sudden changes in heat conductivity and in viscosity. The onset of a localised excitation, or hot spot formation, may therefore set in rather suddenly as a function of energy. Another recent calculation suggests[44] a shortening of the mean free path at approximately 30 MeV/nucleon.

A relevant study is the production of spectator fragments in high energy heavy ion collisions.[45] Such fragments emerge travelling close to beam velocity with a dispersion in momentum determined by the zero point motion of the fragment in the parent projectile, i.e.

$$\sigma^2 = \sigma_0^2 \frac{F(A - F)}{A - 1}$$

where σ is the momentum dispersion, F, A are the mass numbers of fragment and projectile respectively, and $\sigma_0 = P_F/\sqrt{5}$ in the case where the zero point motion is determined by Fermi motion. In Figure 17 the plot of σ_0 obtained[46] from

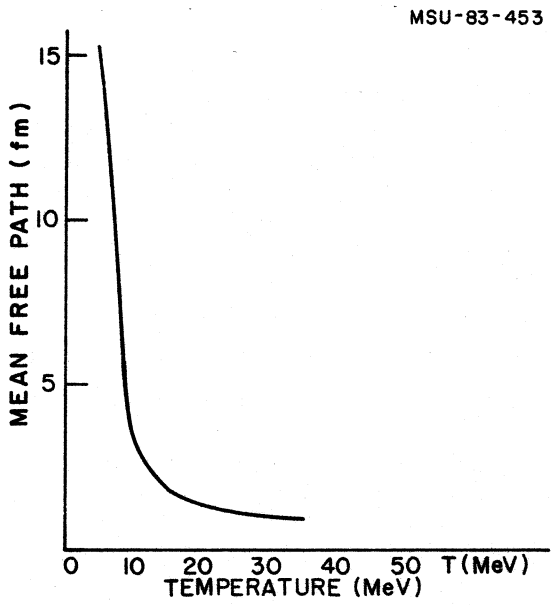

Figure 16. The temperature dependence of the nuclear mean free path. The significant change at T ≅ 10 MeV is associated with the change of mean free path in liquid and gaseous media

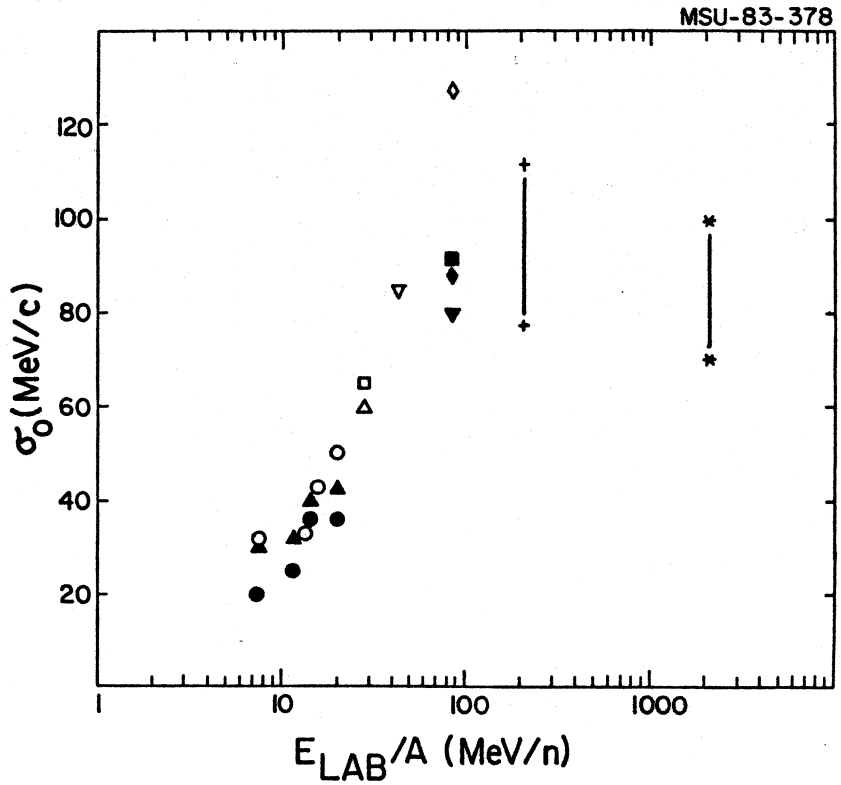

Figure 17. A compilation of several independent measurements of the reduced momentum width parameter σ_0. A large number of such width measurements have been made at 213 and 2100 MeV/nucleon, and the figure illustrates the full range of the results. There is a tendency for a limiting value of σ_0 to set in at incident energies above 50 MeV/nucleon.

a variety of fragments produced in fragmentation of projectiles ranging from ^{12}C to ^{40}Ar at incident energies up to 2 GeV/nucleon shows that an energy independent limit for $\sigma_0 \cong 90$ MeV/c appears to be established at incident energies beyond $\cong$ 50 MeV/nucleon. According to the participant-spectator model, this could signal the emergence of the spectator picture with an implied onset of the complementary participant localisation. If such an interpretation is substantiated, the energy region of 50 MeV/nucleon may be identifiable with the shortening of the mean free path as a result of the liquid-gas phase transition. Due to critical opalescence it is even possible that in the vicinity of the critical temperature the mean free path may also be influenced by the fluctuations between liquid and gas phases. In macroscopic liquids,[47] a small change of temperature, by as little as a fraction of a degree away from the critical point, can cause the substance to change from being almost opaque to almost colorless. Although no such sharp changes are expected in a finite nuclear system, it is conceivable that some vestige of the phenomenon could persist, and indeed a similar shortening of the mean free path due to critical opalescence has been considered in the case of a phase transition to a pion condensate.[47]

b) Exotic Phenomena

The existence of fragments produced in relativistic heavy ion collisions with interaction lengths much shorter than normal is a topic of great current interest.[49] Among the many possible explanations put forward, some of which have been discussed at this conference, there is one that is closely related to the equation of state in regions of low temperature and density such as we have been discussing. In this domain, cluster formation becomes very important, whereas at high density they are supressed by the Mott blocking mechanism.[50] This blocking--itself in the nature of a critical phenomenon--is mediated by the surrounding hot medium which alters the effective binding energy of the clusters to such an extent that the respective bound states merge into the continuum. The density beyond which clustering is no longer possible is called the "Mott density" and it depends on the velocity of the clusters relative to the surrounding matter. Clusters that move with high velocity are less severely degraded, since the quenching arises essentially from Pauli blocking.

Recent calculations suggest[51] that at very low densities, α-cluster formation may give rise to a new metastable phase. We see from Figure 18 that this region sets in at densities of 1/10 to 1/15 of normal density for temperatures of T $\cong$ 2-5 MeV. It develops where the pressure once again crosses zero, corresponding to a stable point on the phase diagram (compare Figure 2). The new region of metastability is shown by the hatching in Figure 19 and disappears at temperatures beyond 12 MeV. This behavior could allow the existence of a low density isomer with a radius much larger than normal nuclei. The authors of Ref. 51 point out that the formation of such α-particle matter may be identifiable with anomalons, although they caution that more detailed estimates of lifetime and the balance of surface and Coulomb energies are necessary to confirm the hypothesis.

The above results, together with the other phenomena discussed in this paper, serve to remind us that the low density and temperature behavior of the equation of state may be a source of interesting new phenomena--like the high density and temperature counterparts. The information provided may also give

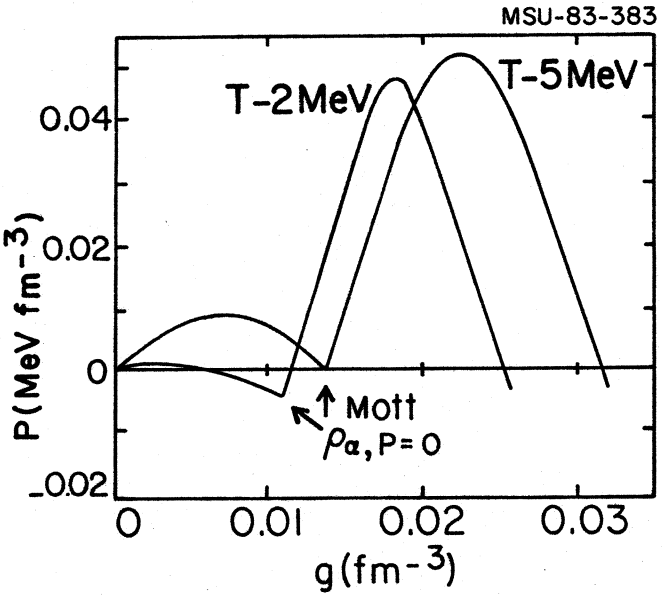

Figure 18. A possible behavior of the equation of state for nuclear matter at very low densities, in which the existence of a new metastable phase determined by clustering effects is predicted. The points labelled $\rho_{\alpha,p}^{MOTT}$ correspond to critical densities beyond which Mott blocking prevents α-cluster formation for zero relative momentum of the clusters relative to the surrounding matter.

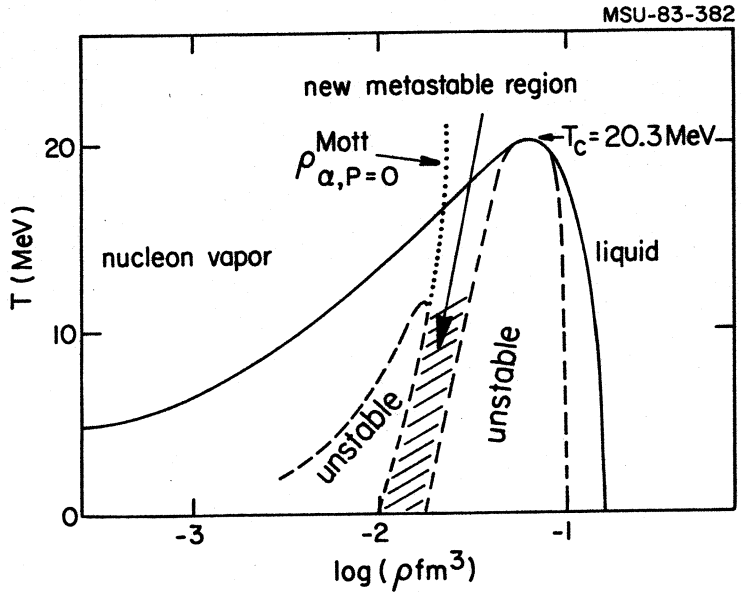

Figure 19. An alternative representation of the phase diagram for nuclear matter showing the coexistence region as well as a predicted new metastable region of α-condensed matter.

insight into other more exotic types of phase transitions, for example to the quark-gluon plasma state expected to be formed when the individual hadron quark bags are forced to overlap by increasing the density or temperature of hadronic matter to high values. Figure 20 gives[52] a P-V diagram for this transition in which three regions are distinguished. There is a hadronic gas region where the pressure rises with reduction in the volume. Eventually the individual hadrons begin to cluster, reducing the Boltzmann pressure since a smaller

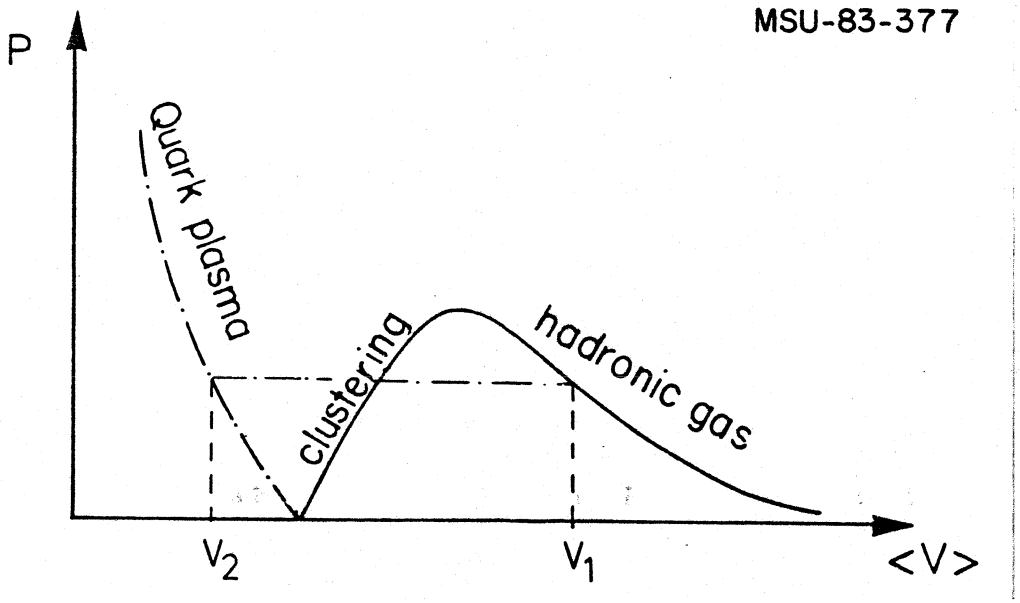

Figure 20. A P-V diagram for hadronic matter. At high densities a phase transition to a quark-gluon plasma is possible. The diagram has a close resemblance to that for the liquid-gas phase transition represented in Figures 2 and 3 for nuclear matter.

number of particles are then present. When the quark-gluon plasma phase is reached the pressure rises again since thereafter only the hadronic constituents are compressed. Clearly this diagram bears a close similarity to Figure 3 which dealt with the analogous problem of liquid condensation from the gas phase. Indeed, many of the problems surrounding the description and the establishment of a phase transition may be rather similar in the two cases--problems, for example, of the time required to establish the transition, the question of the validity of hydrodynamical descriptions of the collision, and so on.

c) Astrophysical Implications

Finally, we mention briefly the interest for astrophysical processes[53,54] of liquid-gas phase phenomena. A well known example of two-phase equilibrium occurs in the crust of neutron stars at temperatures of less than 1 MeV. Also in supernovae, when the inward implosion of collapse is reversed to become an explosion, it is also believed that densities comparable to those in neutron stars are attained with temperatures of 5 to 10 MeV. An understanding of the behavior of matter under those conditions may become possible through studies of nuclear collisions of the type we have discussed in this paper.

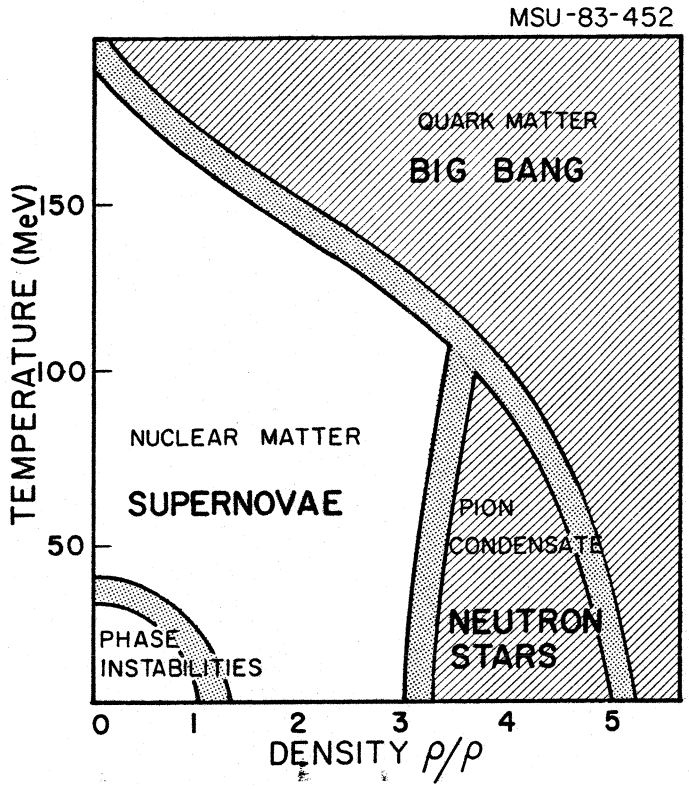

Figure 21. A temperature-density phase diagram for nuclear and hadronic matter. In addition to the exotic phases of quark and pion condensed matter conjectured to occur at high temperature and density, a region of phase instabilities at low temperature and density discussed in this paper is indicated. Each region of phase transition bears a close connection with astrophysical phenomena.

A perspective on the role of the regions of density and temperature we have been discussing is provided by Figure 21. In addition to the three phases of Quark Matter, Pion Condensate, and Nuclear Matter usually displayed, we add an additional region of phase transition, where liquid-gas mechanical instabilities, Mott transitions, and α-condensation may develop. As indicated on the diagram each phase bears a relation to astrophysical phenomena for which the unusual conditions of temperature and density may now become reachable in the laboratory. Thus, while quark-matter may give us our only glimpse of the conditions of matter in the earliest moments of the birth of our Universe, the state of pion condensation--if observed--would simulate conditions prevailing in neutron stars and finally the liquid-gas phase is of direct relevance to supernovae.

6. Conclusion

This paper has dealt with the possibility of investigating critical phenomena in nuclear systems, with particular emphasis on the liquid-gas and mechanical instabilities which can develop at a critical temperatere or at a critical incident energy. Although the phenomena are frequently discussed

and incorporated into calculations of neutron stars and supernovae, the possibility of realising the critical conditions during the evolution of a nuclear collision has only recently been recognised. A study of the approach towards the critical condition can yield information on the temperature dependence of nuclear properties, such as the surface tension. Apart from the intrinsic interest in these phenomena, the phase instabilities may have general implications for the relevance of hydrodynamical concepts in heavy ion collisions and for the localisation of energy deposition through the shortening of the mean free path. The increased interest in the low temperature and low density behavior of the equation of state for nuclear matter has also led to more exotic speculation, for example the creation of metastable phases of α-clustered matter at very low densities, which may be relevant to anomalons. It is also plausible that many of the criteria required for the creation of exotic phases of nuclear matter at high density and temperature, such as the quark-gluon plasma, may be illustrated by phase transitions of the liquid-gas type, the existence of which is based on more accepted knowledge of the equation of state. In particular, questions of time scales and of hydrodynamical behavior are quite pertinent in both cases.

At present there is only sketchy evidence for the existence of critical phenomena of the type we have discussed. The most compelling evidence comes from studies of proton-induced heavy fragment production from a target. Some of the new accelerators will permit new studies of critical phenomena by providing beams of heavy ions over the critical region from 20 to 200 MeV/nucleon. It will take several years for these systematic studies to be completed, because, as we know,

Science moves but slowly, slowly,
creeping on from point to point

Alfred, Lord Tennyson, Locksley Hall

Acknowledgments

I am grateful to many colleagues for discussions, ideas, and data pertaining to this paper. In particular I wish to thank S. Angius, N. Anantaraman, G.F. Bertsch, C.B. Chitwood, M.V. Curtin, G.M. Crawley, D.J. Fields, C.K. Gelbke, B. Hasselquist, B.V. Jacak, J. Kupstas, W.G. Lynch, A.D. Panagiotou, P.J. Siemens, H. Stöcker, H. Toki, B.M. Tsang, H. Utsunomiya, and G.D. Westfall.

My thanks go to Carol Cole for rapid preparation of the manuscript, and to M. Blosser, M. Johnson, and O. McHarris for the illustrations.

This work was supported by the National Science Foundation under Grant No. PHY80-17605.

References

1. M. Gyulassy in Proceedings of the International Conference on Nucleus-Nucleus Collisions (Michigan State University, 1982), eds. G.F. Bertsch, C.K. Gelbke, and D.K. Scott, Nucl. Phys. A400, 31C (1983).
2. H.J. Specht, ibid., p. 43C.
3. H. Satz, ibid., p. 541C.

4. H. Stöcker, J.A. Maruhn, and W. Greiner, Phys. Rev. Lett. 44, 725 (1980).
5. W.A. Kupper, G. Wegmann, and E.R. Hilf, Ann. of Phys. 88, 454 (1974).
6. B. Friedman and V.R. Phandaripande, Nucl. Phys. A361, 502 (1981).
7. D.Q. Lamb, J.M. Lattimer, C.J. Pethick, and D.G. Ravenhall, Phys. Rev. Lett. 41, 1623 (1978); Nucl. Phys. A360, 459 (1981).
8. P. Danielewicz, Nucl. Phys. A314, 465 (1979).
9. M. Barranco and J.R. Buchler, Phys. Rev. C22, 1729 (1980).
10. H. Schulz, L. Munchow, G. Röpke, and H. Schmidt, Phys. Lett. 119B, 12 (1982).
11. M.W. Curtin, H. Toki, and D.K. Scott, Phys. Lett. 123B, 289 (1983).
12. H. Jacaman, A.J. Mekjian, and L. Zamick, Phys. Rev. C27, 2782 (1983).
13. H. Stöcker et al., Proc. of the Int. Conf. on Nucleus-Nucleus Collisions (Michigan State University, 1982), eds. G.F. Bertsch, C.K. Gelbke, and D.K. Scott, Nucl. Phys. A400, 63C (1983).
14. G.F. Bertsch and P.J. Siemens, Phys. Lett. 126B, 9 (1983).
15. G.F. Bertsch and J. Cugnon, Phys. Rev. C24, 2514 (1981).
16. F. Serr, G. Bertsch, and J.P. Blaizot, Phys. Rev. C22, 922 (1980).
17. P. Bonche, S. Koonin, and J. Negele, Phys. Rev. C13, 1226 (1976).
18. J.S. Blakemore in Solid State Physics (W.B. Saunders, Philadelphia, 1974), p. 110.
19. D.K. Scott in Dynamics of Heavy Ion Collisions, eds. N. Cindro, R.A. Ricci, and W. Greiner (North Holland, Amsterdam, 1981), p. 241 and references therein.
20. S. Nagamiya et al., Phys. Rev. C24, 971 (1981).
21. H. Bohning, Proc. of the Int. Conf. on Nuclear Reactions Induced by Heavy Ions, eds. R. Bock and W.R. Hering (North Holland, Amsterdam, 1970), p. 633.
22. M.W. Curtin, H. Toki, and D.K. Scott, Michigan State University Cyclotron Laboratory Preprint MSUCL-426.
23. D.H. Youngblood et al., Phys. Rev. C23, 1997 (1981).
24. R.E.L. Green and R.G. Korteling, Phys. Rev. C22, 1594 (1980) and references therein.
25. K. Aleklett, W. Loveland, P.L. McGaughey, K.J. Moody, R.M. McFarland, R.H. Kraus, Jr., and G.T. Seaborg, Preprints of Contributed Papers to the 6th High Energy Heavy Ion Study and 2nd Workshop on Anomalons (June 1983), Lawrence Berkeley Laboratory Publication LBL-16281, p. 38.
26. S. Bohrmann, J. Hüfner, and M.C. Nemes, Max Planck Institute, Heidelberg Preprint MPIH 1982-V16.
27. J.E. Finn, S. Agarwal, A. Bujak, J. Chuang, L.J. Gutay, A.S. Hirsch, R.W. Minich, N.T. Porile, R.P. Scharenberg, B.C. Stringfellow, and F. Turkot, Phys. Rev. Lett. 49, 1321 (1982).
28. R.W. Minich, S. Agarwal, A. Bujak, J. Chuang, J.E. Finn, L.J. Gutay, A.S. Hirsch, N.T. Porile, R.P. Scharenberg, B.C. Stringfellow, and F. Turkot, Phys. Lett. 118B, 458 (1982).
29. M. Fisher, Physics V3, 255 (1967).
30. P.J. Siemens, Preprint 1983, submitted to Nature.
31. H. Stöcker and J. Burzlaff, Nucl. Phys. A202, 265 (1973).
32. G. Sauer, H. Chandra, and U. Mosel, Nucl. Phys. A264, 221 (1976).
33. S. Das Gupta and A.Z. Mekjian, Phys. Reports 72, 131 (1981) and references therein.
34. S. Angius, M.Sc. Thesis, Michigan State University 1982; S. Angius and D.K. Scott, Annual Report (Michigan State University Cyclotron Laboratory 1981-1982), p. 24.

35. S. Nagamiya, Proc. of Int. Conf. on Nucleus-Nucleus Collisions (Michigan State University, 1982), eds. G.F. Bertsch, C.K. Gelbke, and D.K. Scott, Nucl. Phys. A400, 399C (1983).
36. C.B. Chitwood, D.J. Fields, C.K. Gelbke, W.G. Lynch, A.D. Panagiotou, M.B. Tsang, H. Utsunomiya, and W.A. Friedman, Phys. Lett. B, to be published.
37. W. Friedman and W.G. Lynch, Phys. Rev. C28, 16 (1983).
38. W. Friedman and W.G. Lynch, Phys. Rev. C28, 950 (1983).
39. H.H. Gutbrod, A.I. Warwick, and H. Weiman in Selected Aspects of Heavy Ion Collisions (Saclay, 1982), eds. M. Martinot, C. Ngô, and P. Gugenberger (North Holland-Amsterdam, 1982), p. 177C.
U. Lynen et al., ibid., p. 129C.
41. B. Jakobsson, G. Jönson, B. Linquist, and A. Oskarsson, Z. Phys. A307, 293 (1982).
42. J. Kapusta, Preprint, 1983.
43. S.I.A. Garpman, D. Sperber, and M. Zielinska-Pfabe, Nuov. Cim. 57B (1980).
44. B. Sinha, Phys. Rev. Lett. 50, 91 (1983).
45. D.K. Scott in Proc. of the Int. Conf. on Nuclear Physics (Berkeley, 1980), eds. R.M. Diamond and J.O. Rasmussen, Nucl. Phys. A354, 375C (1981).
46. M.J. Murphy and R.G. Stokstad, to be published, and Lawrence Berkeley Laboratory Publication PUB-5078, 1982.
47. H.E. Stanley, Introduction to Phase Transitions and Critical Phenomena (Clarendon Press, Oxford, 1971).
48. H. Stöcker, J. Hofmann, J.A. Maruhn, and W. Greiner, Progress in Particle and Nuclear Physics, Vol. 4 (1980); M. Gyulassy and W. Greiner, Ann. Phys. 109, 485 (1977).
49. W. Heinrich et al. in Proc. of Int. Conf. on Nucleus-Nucleus Collisions (Michigan State University, 1982), eds. G.F. Bertsch, C.K. Gelbke, and D.K. Scott, Nucl. Phys. A400, 315C (1983).
50. G. Röpke, L. Münchow, and H. Schulz, Nucl. Phys. A359, 536 (1982); Phys. Lett. B112, 13 (1982).
51. R. Schulz, G. Röpke, and M. Schmidt, Z. Phys. A310, 139 (1983).
52. J. Rafelski and M. Danos, Perspectives in High Energy Nuclear Collisions, National Bureau of Standards Publication NBSIR 83-2725, 1983, p. 5.
53. G. Baym and C. Pethick, Ann. Rev. Nucl. Sci. 25, 27 (1975).
54. G.E. Brown, H.A. Bethe, and G. Baym, Nucl. Phys. A375, 481 (1982).